École Doctorale des Sciences de l'Environnement d'Île-de-France

Année Universitaire 2016-2017

Modélisation Numérique de l'Écoulement Atmosphérique et Assimilation de Données

Olivier Talagrand

Cours 2

13 Avril 2017

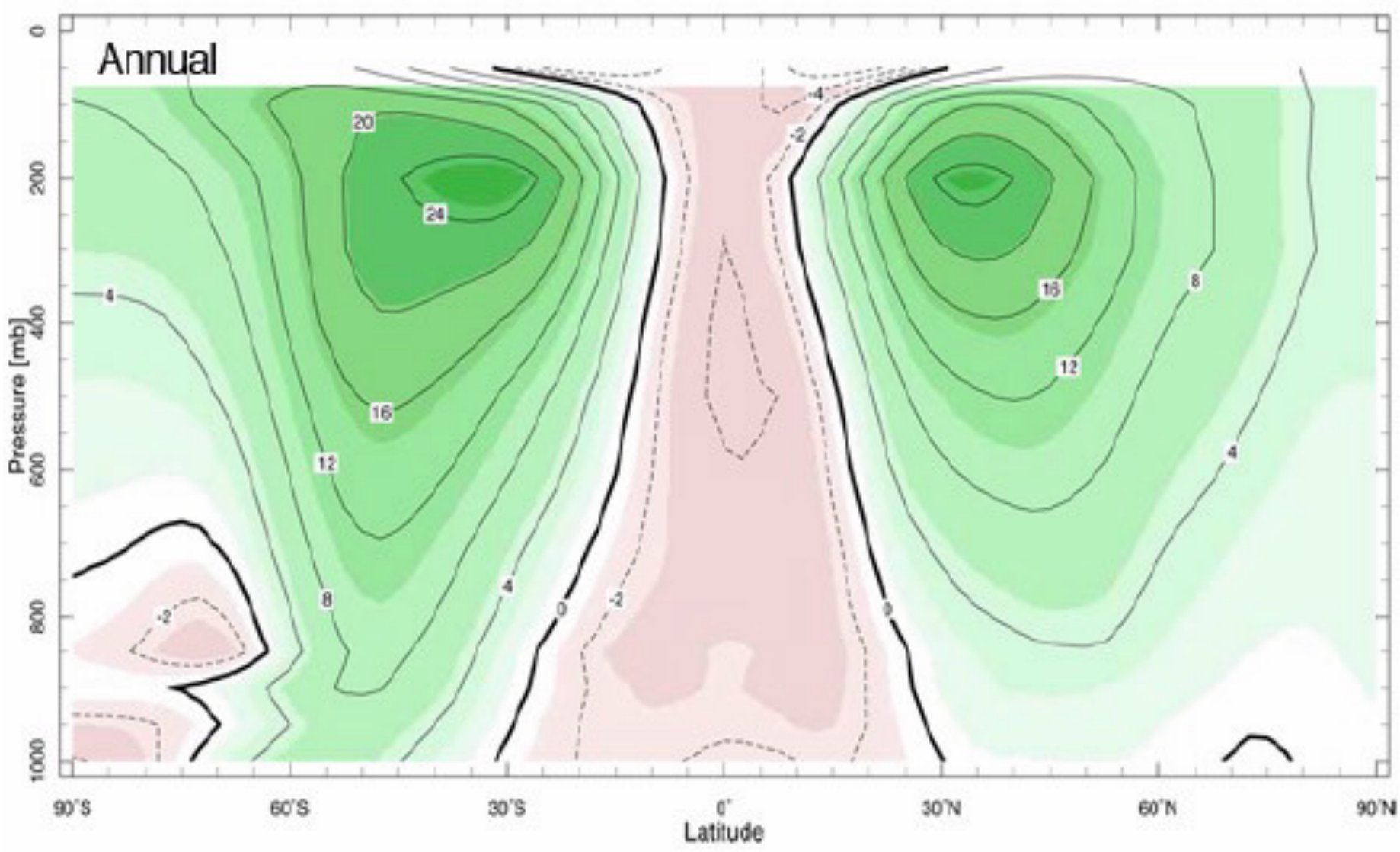

Vent zonal; moyenne longitudinale annuelle ($m.s^{-1}$)
http://paoc.mit.edu/labweb/notes/chap5.pdf,
Atmosphere, Ocean and Climate Dynamics, by J. Marshall and R. A. Plumb,
International Geophysics, Elsevier)

Modèles (semi-)spectraux

$$T(\mu=\sin(\text{latitude}),\ \lambda=\text{longitude}) = \sum_{\substack{0\le n<\infty \\ -n\le m\le n}} T_n^m Y_n^m(\mu,\lambda)$$

où les $Y_n^m(\mu,\lambda)$ sont les *harmoniques sphériques*

$$Y_n^m(\mu,\lambda) \propto P_n^m(\mu)\exp(im\lambda)$$

$P_n^m(\mu)$ est la *fonction de Legendre* de deuxième espèce.

$$P_n^m(\mu) \propto (1-\mu^2)^{\frac{m}{2}} \frac{d^{n+m}}{d\mu^{n+m}}(\mu^2-1)^n$$

n et m sont respectivement le *degré* et l'*ordre* de l'harmonique $Y_n^m(\mu,\lambda)$

$n = 0, 1, \ldots$ $\quad - n \le m \le n$

From Wikipedia, the free encyclopedia

$l = 3$
$m = 0$
$l\text{-}m = 3$

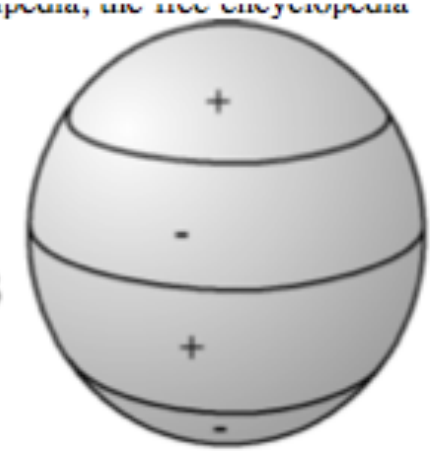

$l = 3$
$m = 1$
$l\text{-}m = 2$

$l = 3$
$m = 2$
$l\text{-}m = 1$

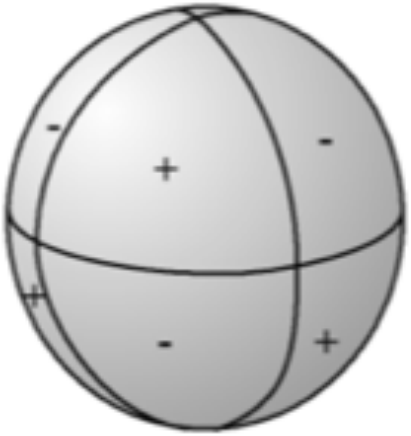

$l = 3$
$m = 3$
$l\text{-}m = 0$

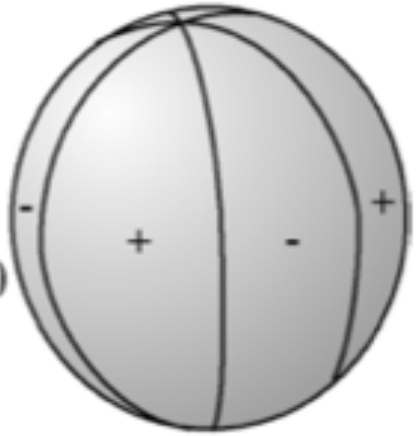

$l = 5$
$m = 2$
$l\text{-}m = 3$

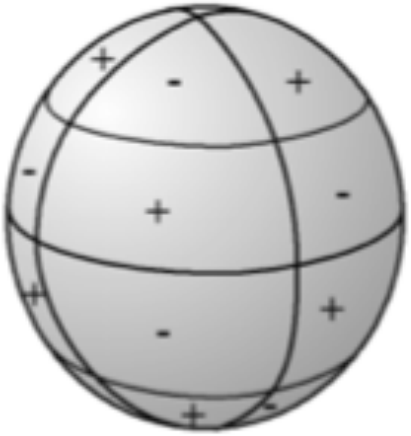

Modèles (semi-)spectraux

Les harmoniques sphériques définissent une base complète orthonormée de l'espace L^2 à la surface S de la sphère.

$$\int_S Y_n^m Y_{n'}^{m'} d\mu d\lambda = \delta_n^{n'} \delta_m^{m'}$$

Relation de Parseval

$$\int_S T^2(\mu,\lambda) d\mu d\lambda = \sum_{\substack{0 \le n < \infty \\ -n \le m \le n}} \left| T_n^m \right|^2$$

Les harmoniques sphériques sont fonctions propres du laplacien à la surface de la sphère

$$\Delta Y_n^m = -n(n+1)Y_n^m$$

Troncature ‘triangulaire’ *TN* ($n \leq N$, $-n \leq m \leq n$) indépendante du choix d’un axe polaire. Représentation est parfaitement homogène à la surface de la sphère

Calculs non linéaires effectués dans l’espace physique (sur grille appropriée, souvent latitude-longitude ‘gaussienne’). Les transformations requises sont possibles à un coût non prohibitif grâce à l’utilisation de Transformées de Fourier Rapides (*Fast Fourier Transforms*, *FFT*, en anglais). Il existe aussi une version rapide des Transformées de Legendre, relatives à la variable μ.

Pressure p, although convenient for writing down the equations, is in fact rather inconvenient because lower boundary is not fixed in (x, y, p)-space.

So-called σ-coordinate. $\sigma \equiv p/p_S$, where p_S is pressure at ground level.

'Hybrid' coordinate.

Lois physiques régissant l'écoulement

- Conservation de la masse

  $D\rho/Dt + \rho \, \mathrm{div}\underline{U} = 0$

- Conservation de l'énergie

  $De/Dt - (p/\rho^2) \, D\rho/Dt = Q$

- Conservation de la quantité de mouvement

  $D\underline{U}/Dt + (1/\rho) \, \underline{\mathrm{grad}}p - \underline{g} + 2 \, \underline{\Omega} \wedge \underline{U} = \underline{F}$

- Equation d'état

  $f(p, \rho, e) = 0$ $\qquad\qquad$ $(p/\rho = rT, e = C_v T)$

- Conservation de la masse de composants secondaires (eau pour l'atmosphère, sel pour l'océan, espèces chimiques, …)

  $Dq/Dt + q \, \mathrm{div}\underline{U} = S$

Temporal discretization. Courant-Friedrichs-Lewy (CFL) condition for stability of explicit schemes

$$\Delta t / \Delta x < \alpha / c$$

where c is phase velocity of fastest propagating (wave) in the system, and α is an $O(1)$ numerical coefficient depending on particular scheme under consideration.

Significance : numerical propagation of signal must be at least as fast as physical propagation.

In hydrostatic atmosphere, fastest propagating wave : gravity wave with largest scale height, $c = \sqrt{(rT)} \approx 300$ $m.s^{-1}$.

$$\Delta x = 30 \text{ km} \quad \Rightarrow \Delta t = 100 \text{ s}$$

The use of *semi-implicit* schemes allows to get rid of the CFL condition, and to use longer timesteps.

In the parlance of the trade, one distinguishes two different parts in models. The ‘dynamics’ deals with the physically reversible processes (pressure forces, Coriolis force, advection, …), while the ‘physics’ deals with physically irreversible processes, in particular the diabatic heating term Q in the energy equation, and also the parameterization of subgrid scales effects.

Numerical schemes have been gradually developed and validated for the ‘dynamics’ component of models, which are by and large considered now to work satisfactorily (although regular improvements are still being made; project *DYNAMICO*, *Dynamical Core on Icosahedral Grid*, Th. Dubos, IPSL).

The situation is different as concerns ‘physics’, where many problems remain (as concerns for instance subgrid scales parameterization, the water cycle and the associated exchanges of energy, or the exchanges that take place in the boundary layer between the atmosphere and the underlying medium). ‘Physics’ as a whole remains the weaker point of models, and is still the object of active research.

5 - SCHEMA DES INTERACTIONS PHYSIQUES DANS LE MODELE

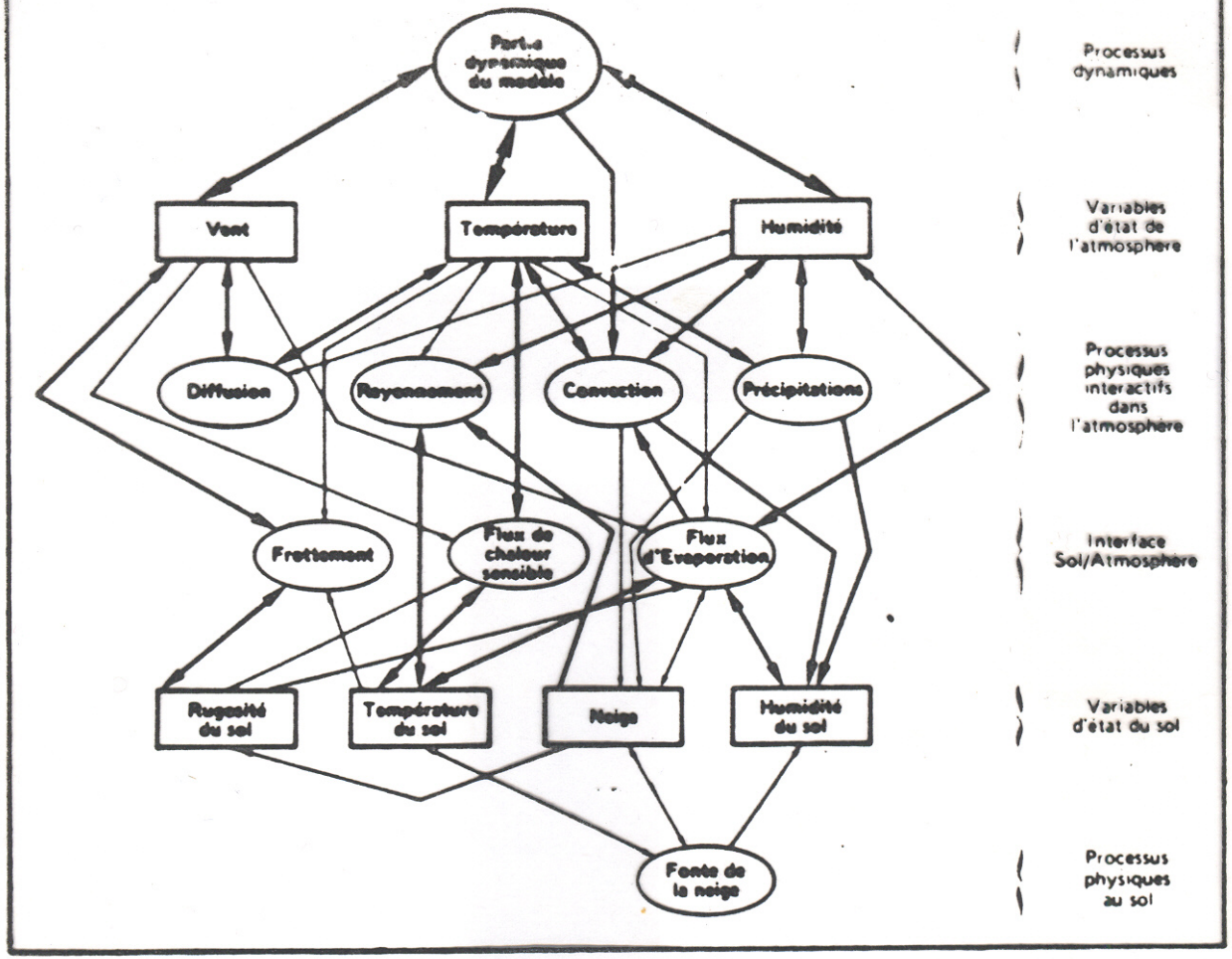

Centre Européen pour les Prévisions Météorologiques à Moyen Terme (CEPMMT, Reading, GB)

(European Centre for Medium-range Weather Forecasts, ECMWF)

Depuis mars 2016 :

Troncature triangulaire TCO1279 / O1280 (résolution horizontale ≈ 9 kilomètres)

137 niveaux dans la direction verticale (0 - 80 km)

Discrétisation en éléments finis dans la direction verticale

Dimension du vecteur d'état correspondant > 10^9

Pas de discrétisation temporelle (schéma semi-Lagrangien semi-implicite): 450 secondes

Wednesday 05 April 2017 0000 UTC ECMWF t+168 VT: Wednesday 12 April 2017 0000 UTC
850 hPa Temperature/500 hPa Geopotential

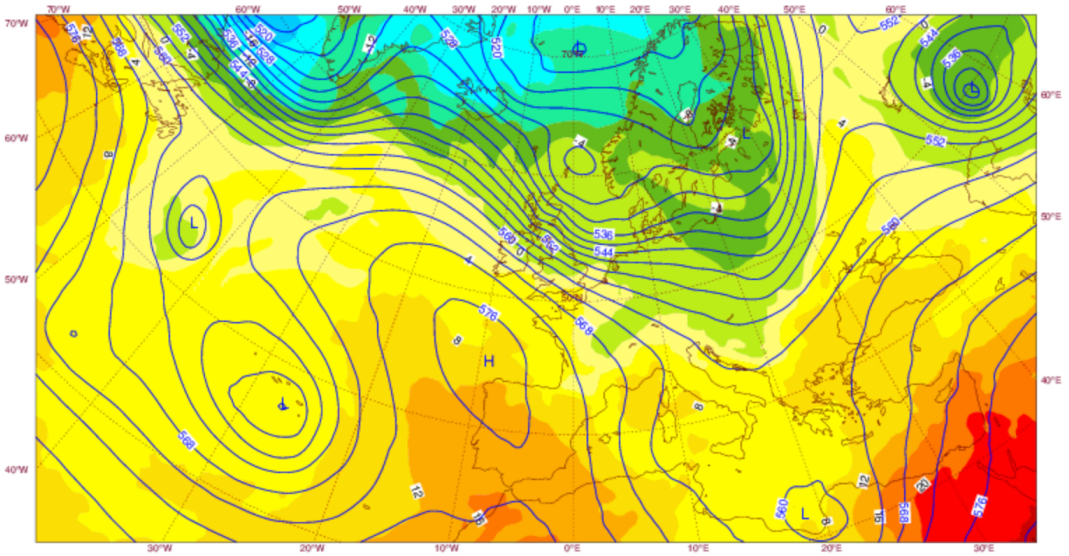

Wednesday 12 April 2017 0000 UTC ECMWF t+0 VT: Wednesday 12 April 2017 0000 UTC
850 hPa Temperature/500 hPa Geopotential

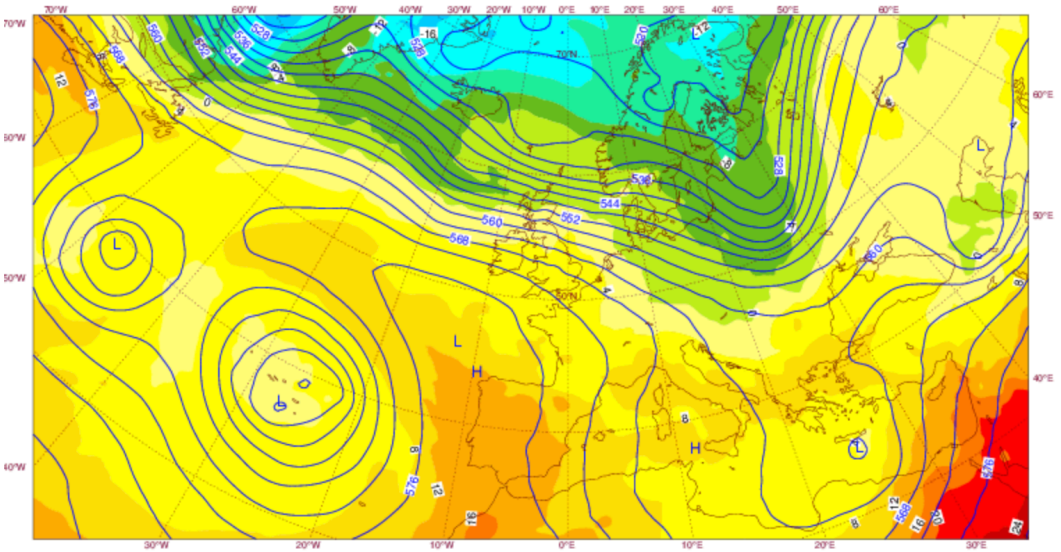

Wednesday 05 April 2017 0000 UTC ECMWF t+0 VT: Wednesday 05 April 2017 0000 UTC
850 hPa Temperature/500 hPa Geopotential

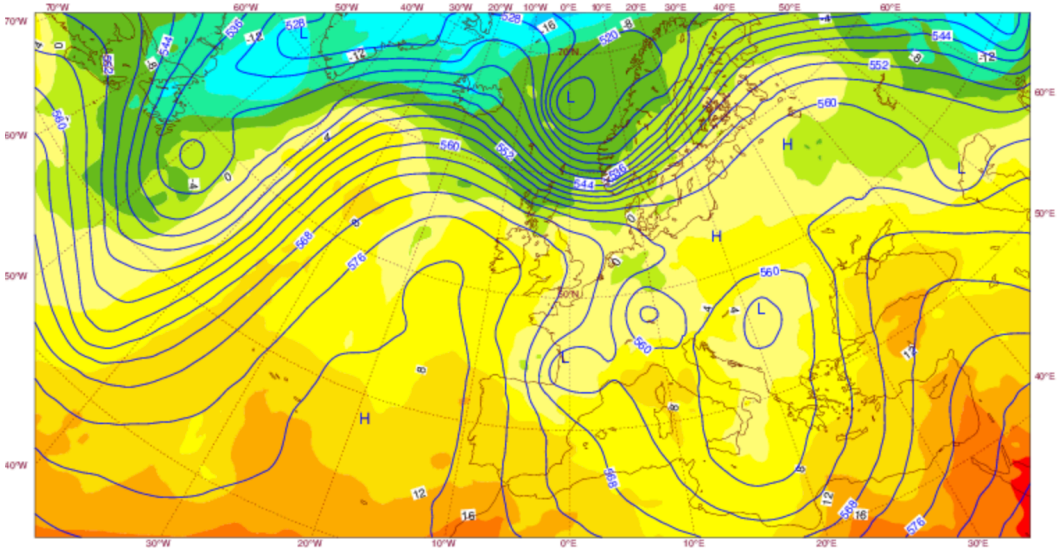

Wednesday 12 April 2017 0000 UTC ECMWF t+0 VT: Wednesday 12 April 2017 0000 UTC
850 hPa Temperature/500 hPa Geopotential

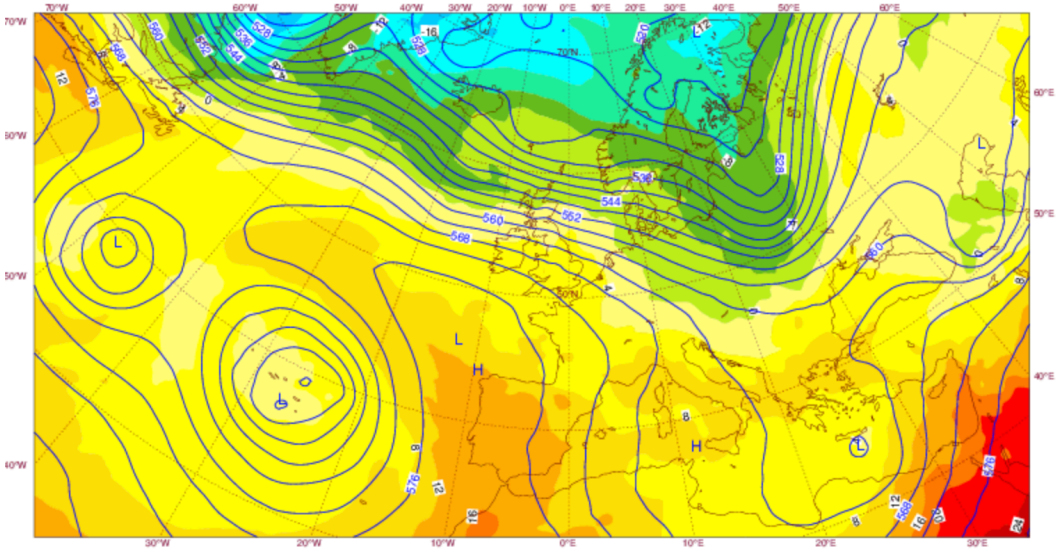

Sunday 10 January 2016 00UTC ©ECMWF Forecast t+168 VT: Sunday 17 January 2016 00UTC
850 hPa Temperature / 500 hPa Geopotential

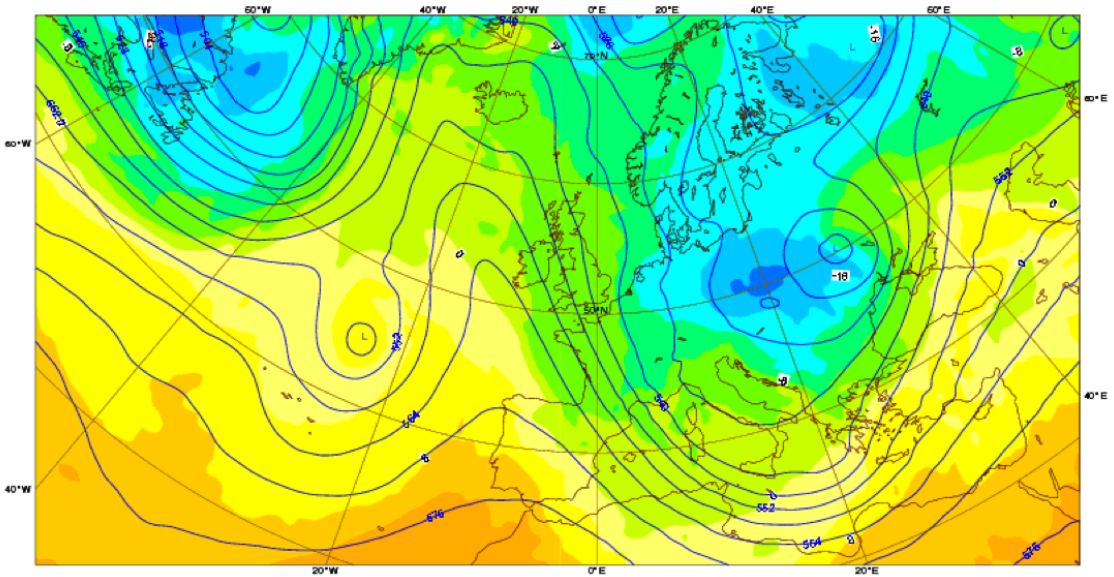

Sunday 17 January 2016 00UTC ©ECMWF Analysis t+000 VT: Sunday 17 January 2016 00UTC
850 hPa Temperature / 500 hPa Geopotential

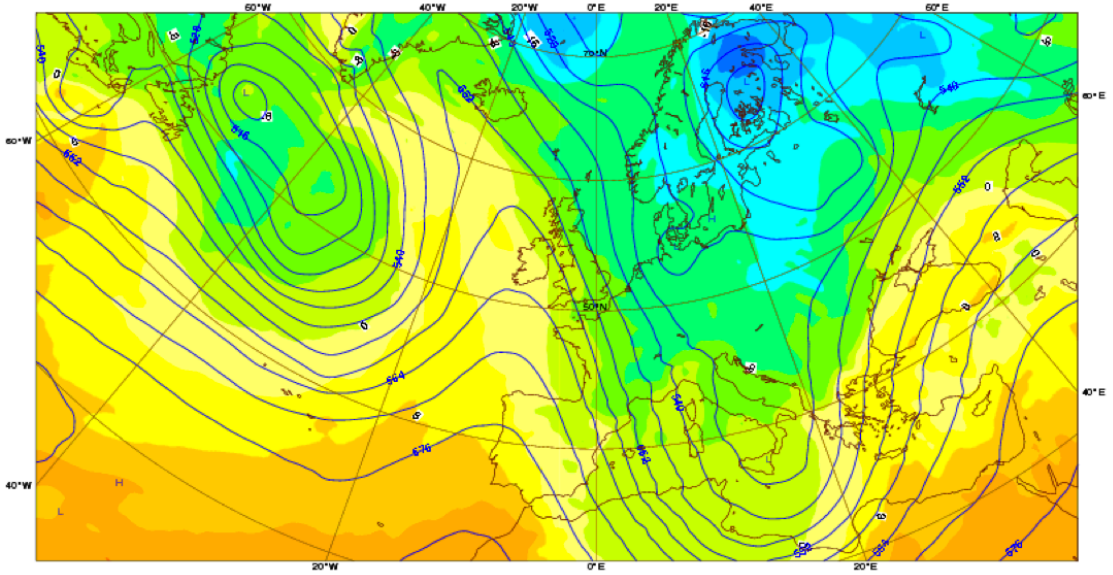

Sunday 10 January 2016 00UTC ©ECMWF Analysis t+000 VT: Sunday 10 January 2016 00UTC
850 hPa Temperature / 500 hPa Geopotential

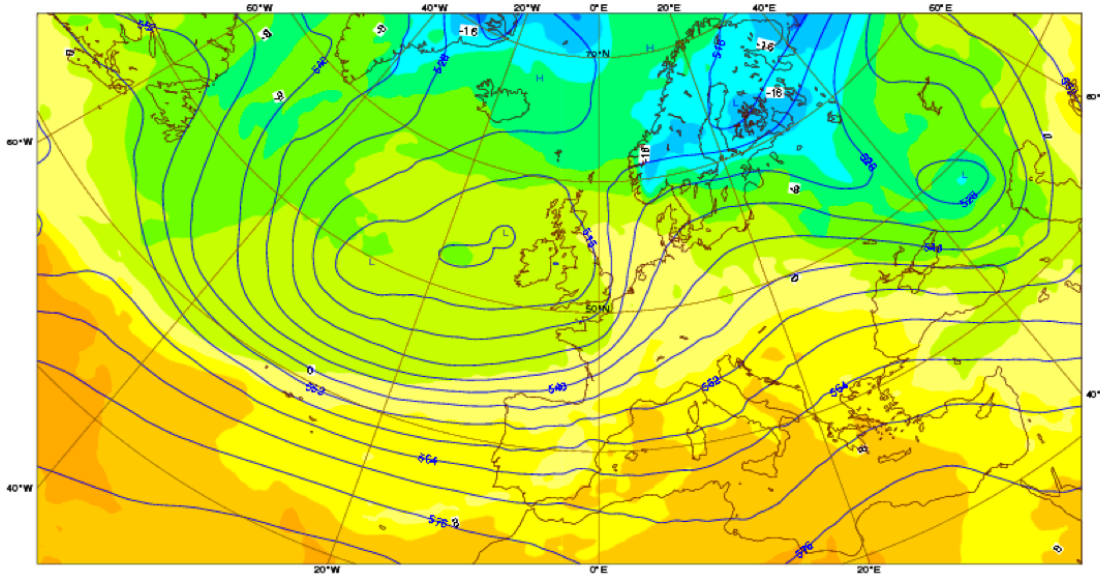

Sunday 17 January 2016 00UTC ©ECMWF Analysis t+000 VT: Sunday 17 January 2016 00UTC
850 hPa Temperature / 500 hPa Geopotential

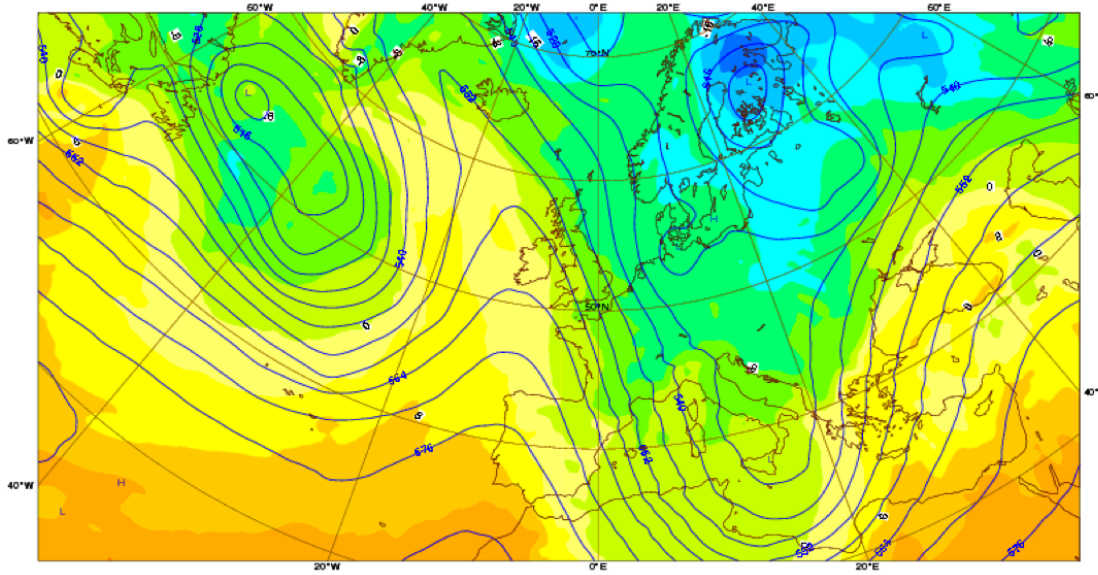

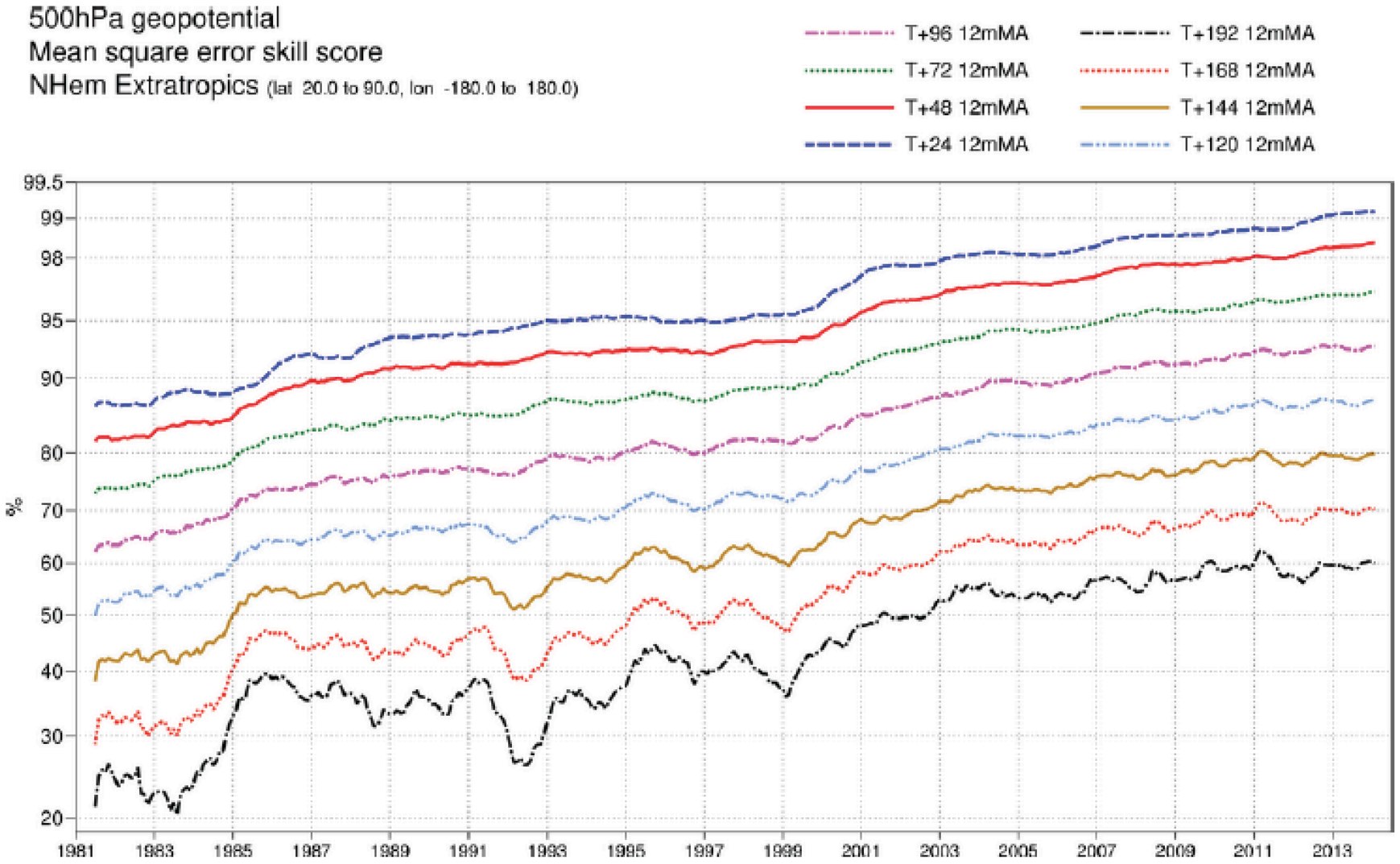

Figure 3: 500 hPa geopotential height mean square error skill score for Europe (top) and the northern hemisphere extratropics (bottom), showing 12-month moving averages for forecast ranges from 24 to 192 hours. The last point on each curve is for the 12-month period August 2013–July 2014.

Persistence = 0 ; climatology = 50 at long range

Initial state error reduction

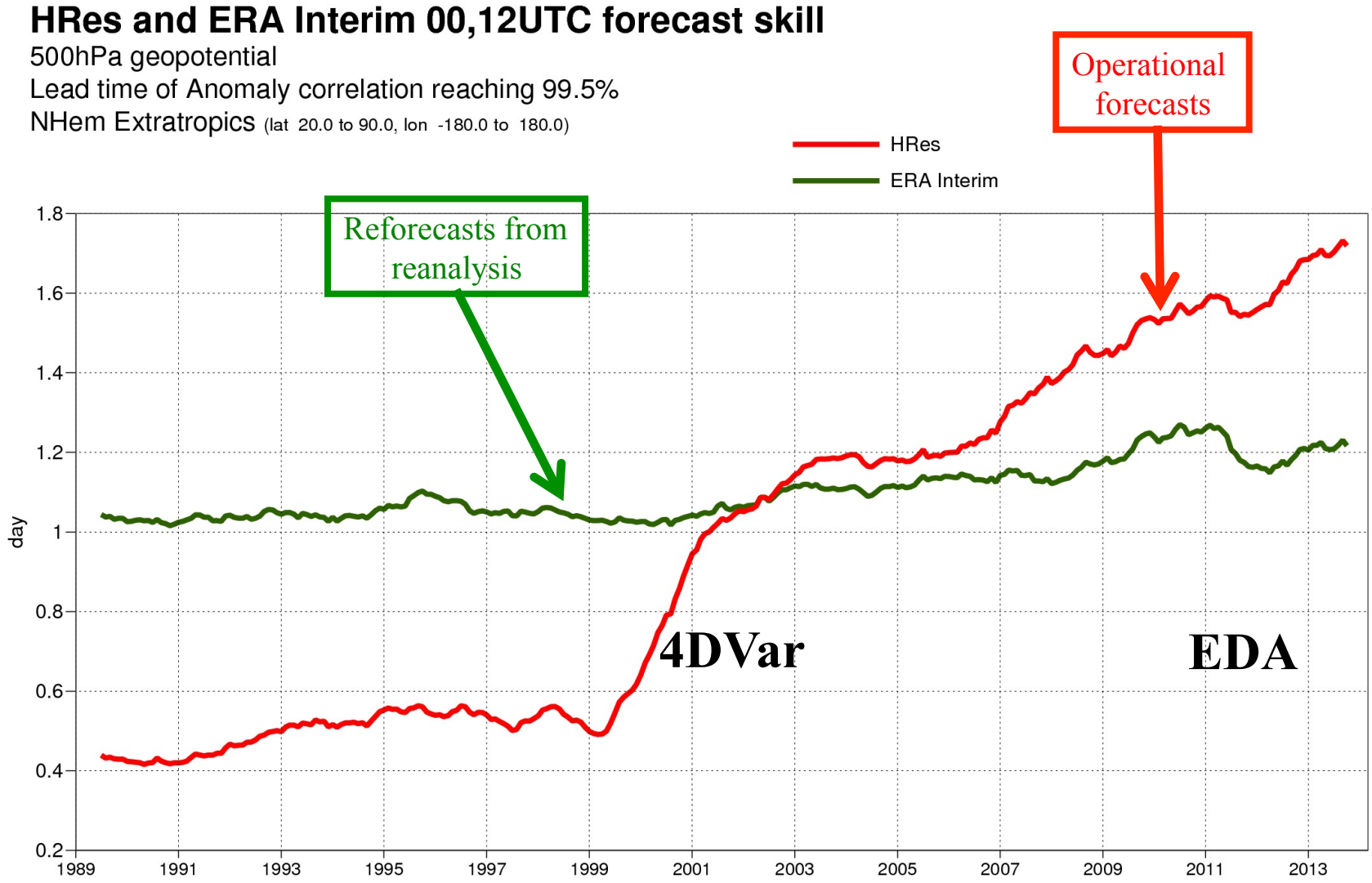

Credit E. Källén, ECMWF

Results extracted from :

Haiden *et al.*, 2016, *Evaluations of ECMWF forecasts, including the 2016 resolution upgrade*, Memorandum Technique 792, CEPMMT, Reading, GB.

Available at the address

http://www.ecmwf.int/sites/default/files/elibrary/2016/16924-evaluation-ecmwf-forecasts-including-2016-resolution-upgrade.pdf

(see also the complete site of ECMWF)

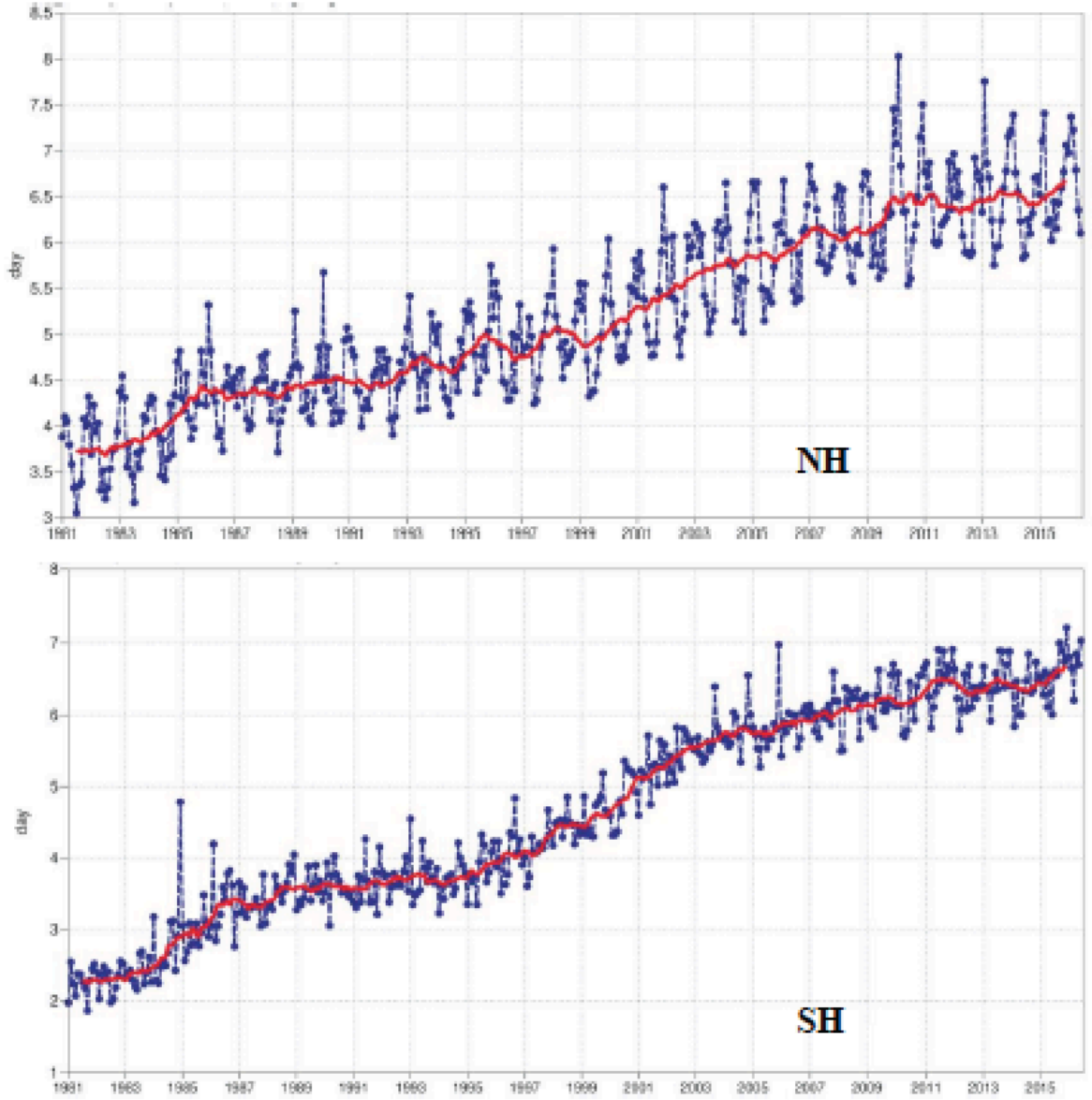

Figure 2: Primary headline score for the high-resolution forecasts. Evolution with time of the 500 hPa geopotential height forecast performance – each point on the curves is the forecast range at which the monthly mean (blue lines) or 12-month mean centred on that month (red line) of the forecast anomaly correlation (ACC) with the verifying analysis falls below 80% for Europe (top), northern hemisphere extratropics (centre) and southern hemisphere extratropics (bottom).

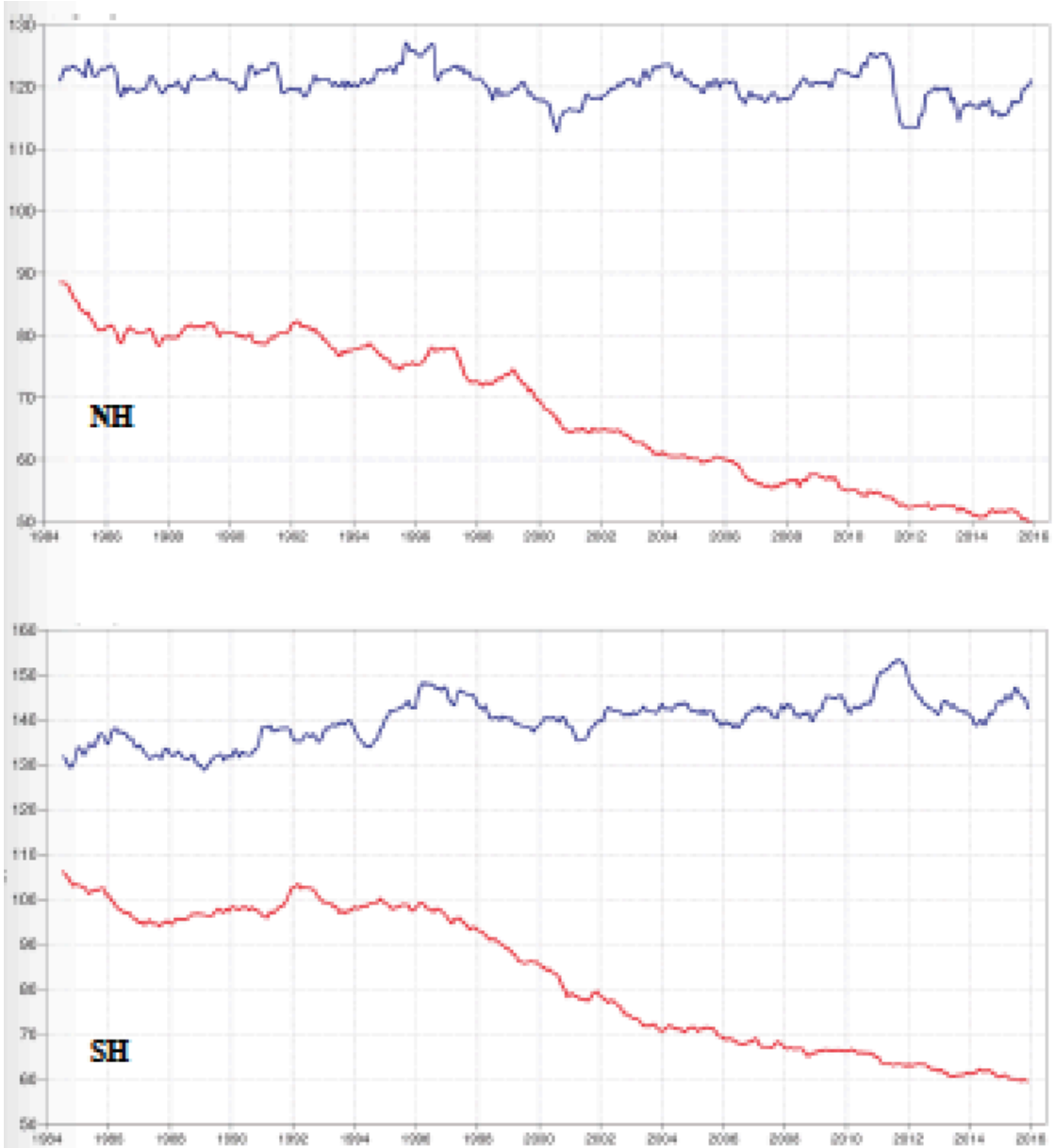

Figure 3: Root mean square (RMS) error of forecasts of 500 hPa geopotential height (m) at day 6 (red), verified against analysis. For comparison, a reference forecast made by persisting the analysis over 6 days is shown (blue). Plotted values are 12-month moving averages; the last point on the curves is for the 12-month period August 2015–July 2016. Results are shown for the northern extra-tropics (top), and the southern extra-tropics (bottom).

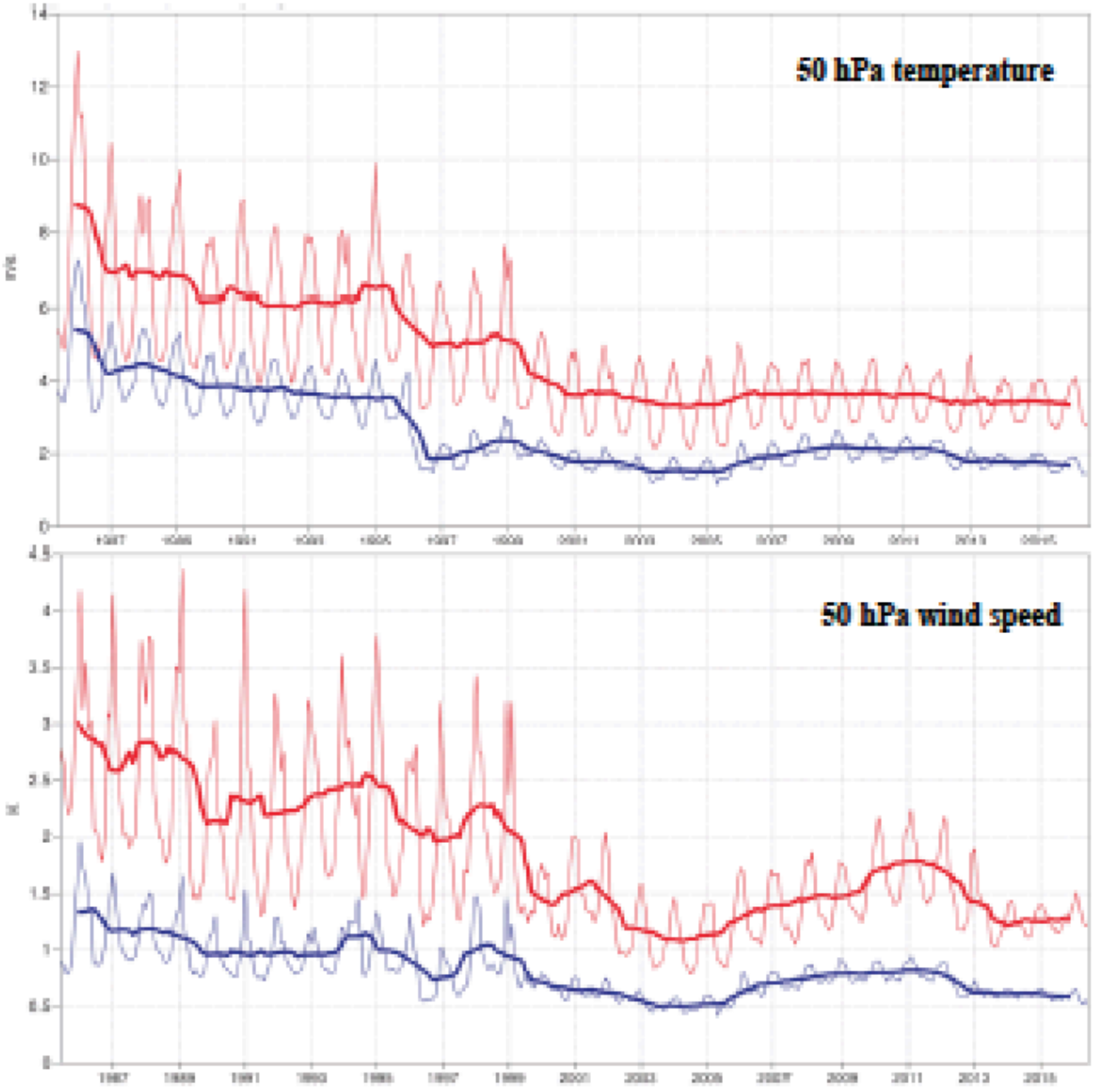

Figure 5: Model scores for temperature (top) and wind (bottom) in the northern extratropical stratosphere. Curves show the monthly average RMS temperature and vector wind error at 50 hPa for one-day (blue) and five-day (red) forecasts, verified against analysis. 12-month moving average scores are also shown (in bold).

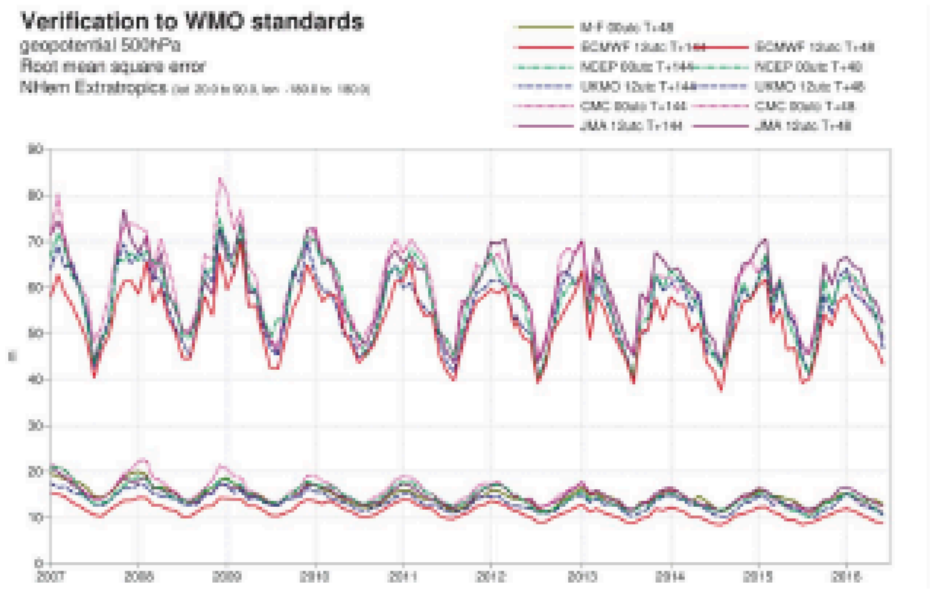

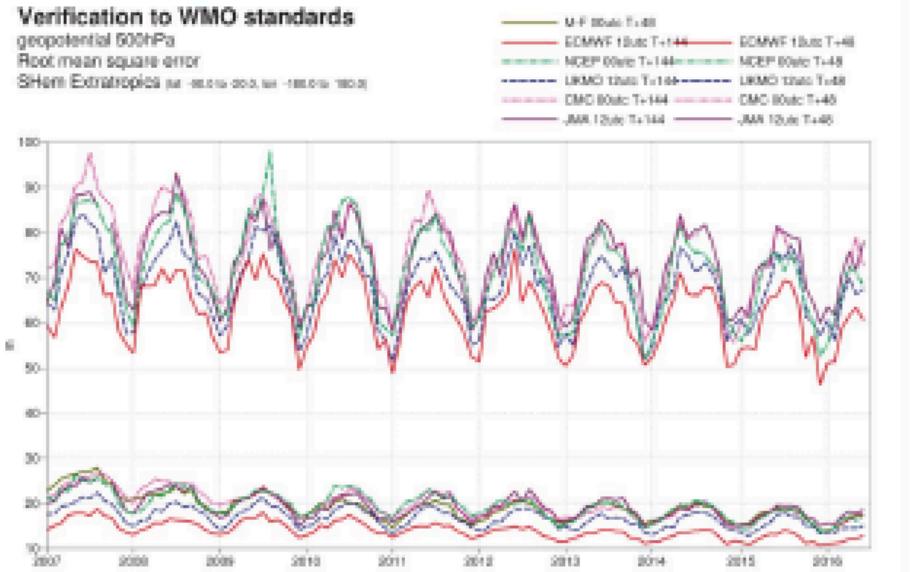

Figure 12: WMO-exchanged scores from global forecast centres. RMS error of 500 hPa geopotential height over northern (top) and southern (bottom) extratropics. In each panel the upper curves show the six-day forecast error and the lower curves show the two-day forecast error. Each model is verified against its own analysis. JMA = Japan Meteorological Agency, CMC = Canadian Meteorological Centre, UKMO = the UK Met Office, NCEP = U.S. National Centers for Environmental Prediction, M-F = Météo France.

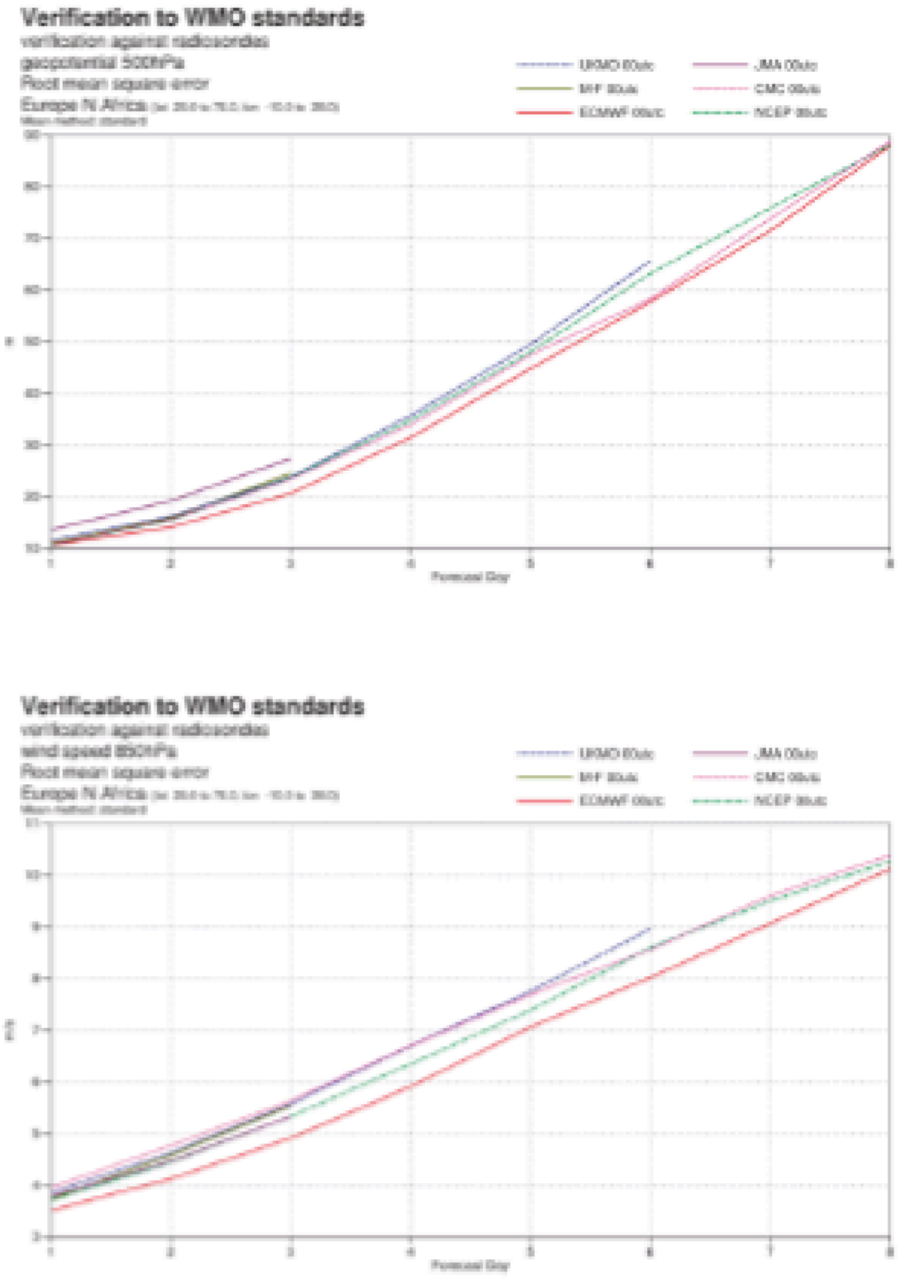

Figure 13: WMO-exchanged scores for verification against radiosondes: 500 hPa height (top) and 850 hPa wind (bottom) RMSerror over Europe (annual mean August 2015–July 2016).

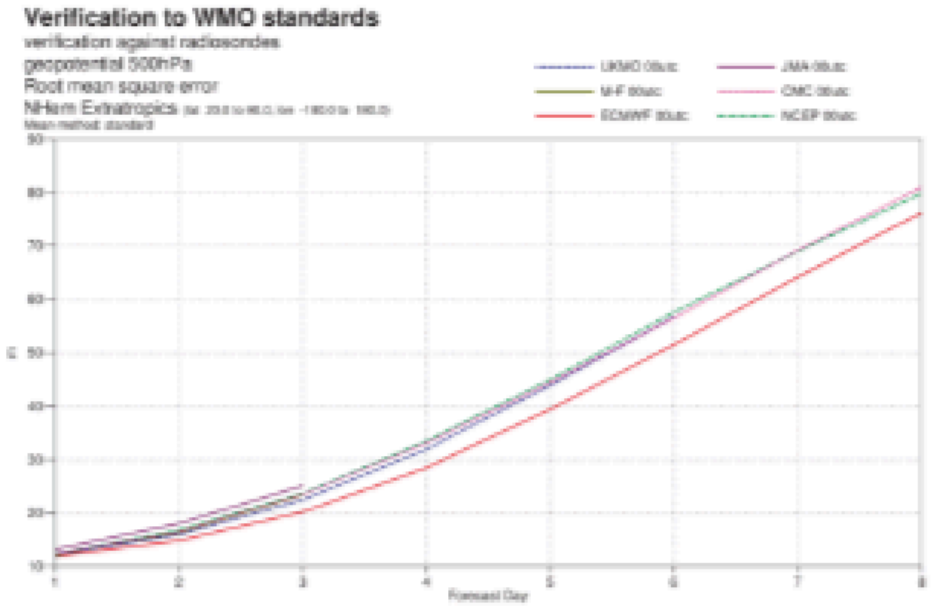

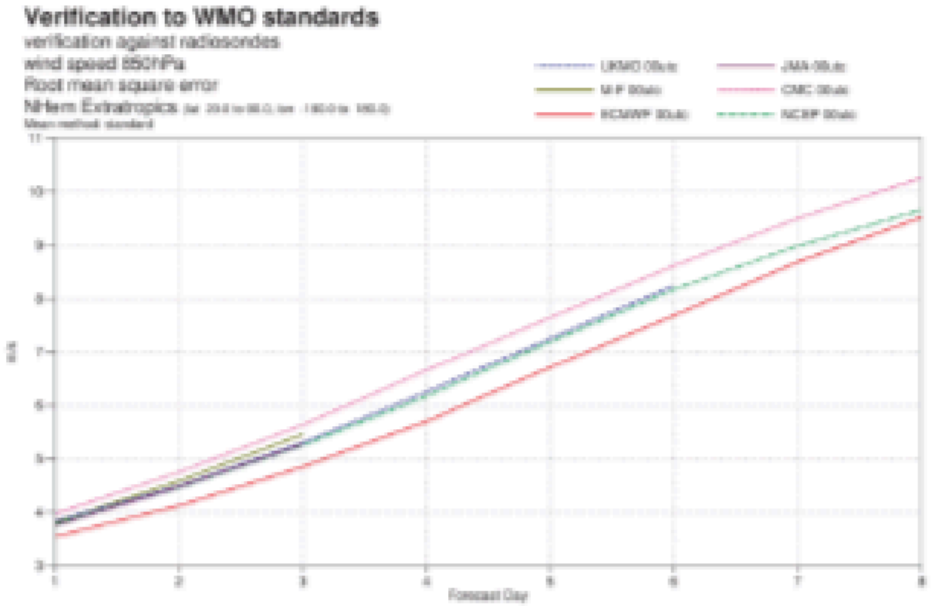

Figure 14: As Figure 13 for the northern hemisphere extratropics.

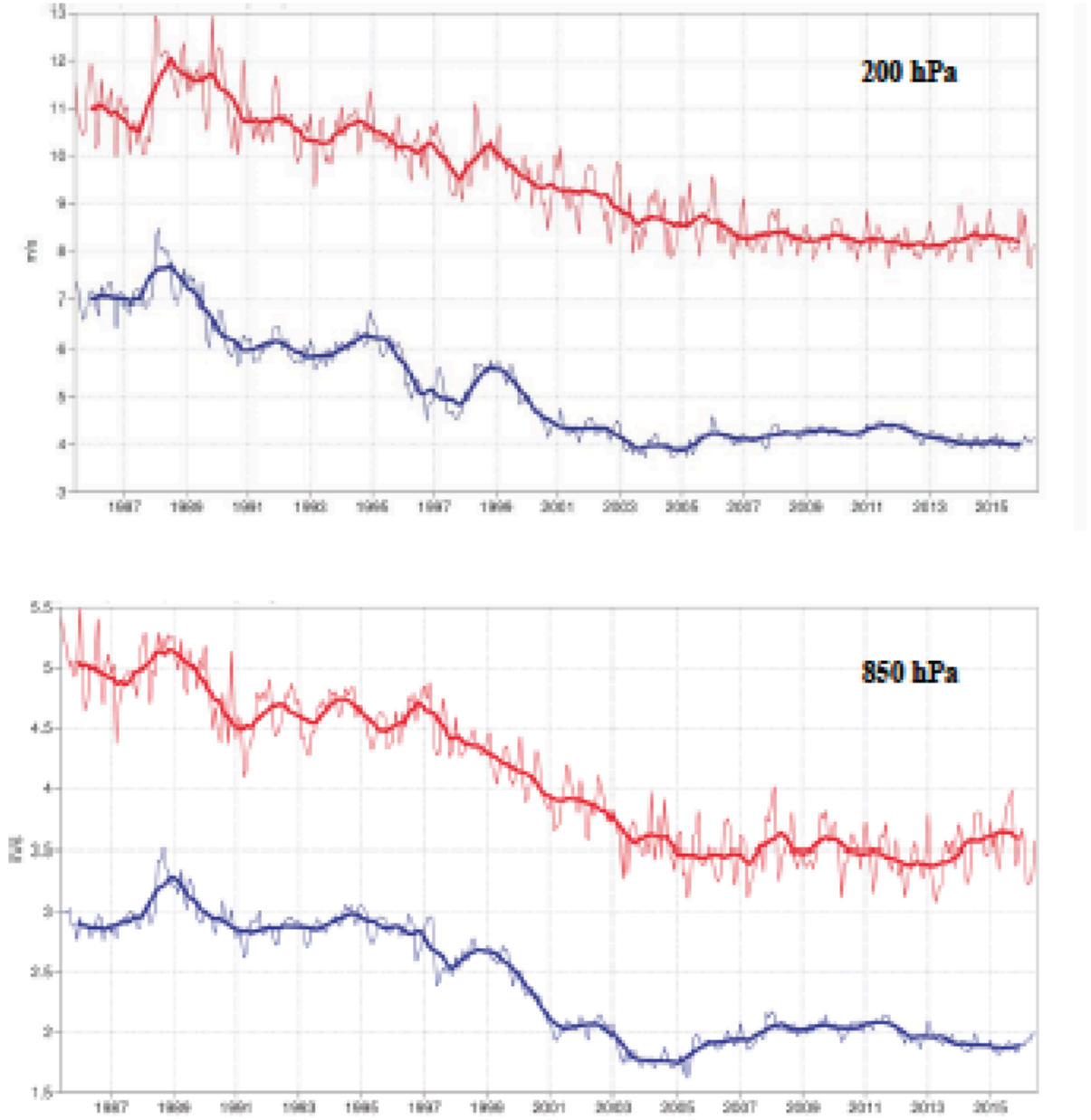

Figure 11: Forecast performance in the tropics. Curves show the monthly average RMS vector wind errors at 200 hPa (top) and 850 hPa (bottom) for one-day (blue) and five-day (red) forecasts, verified against analysis. 12-month moving average scores are also shown (in bold).

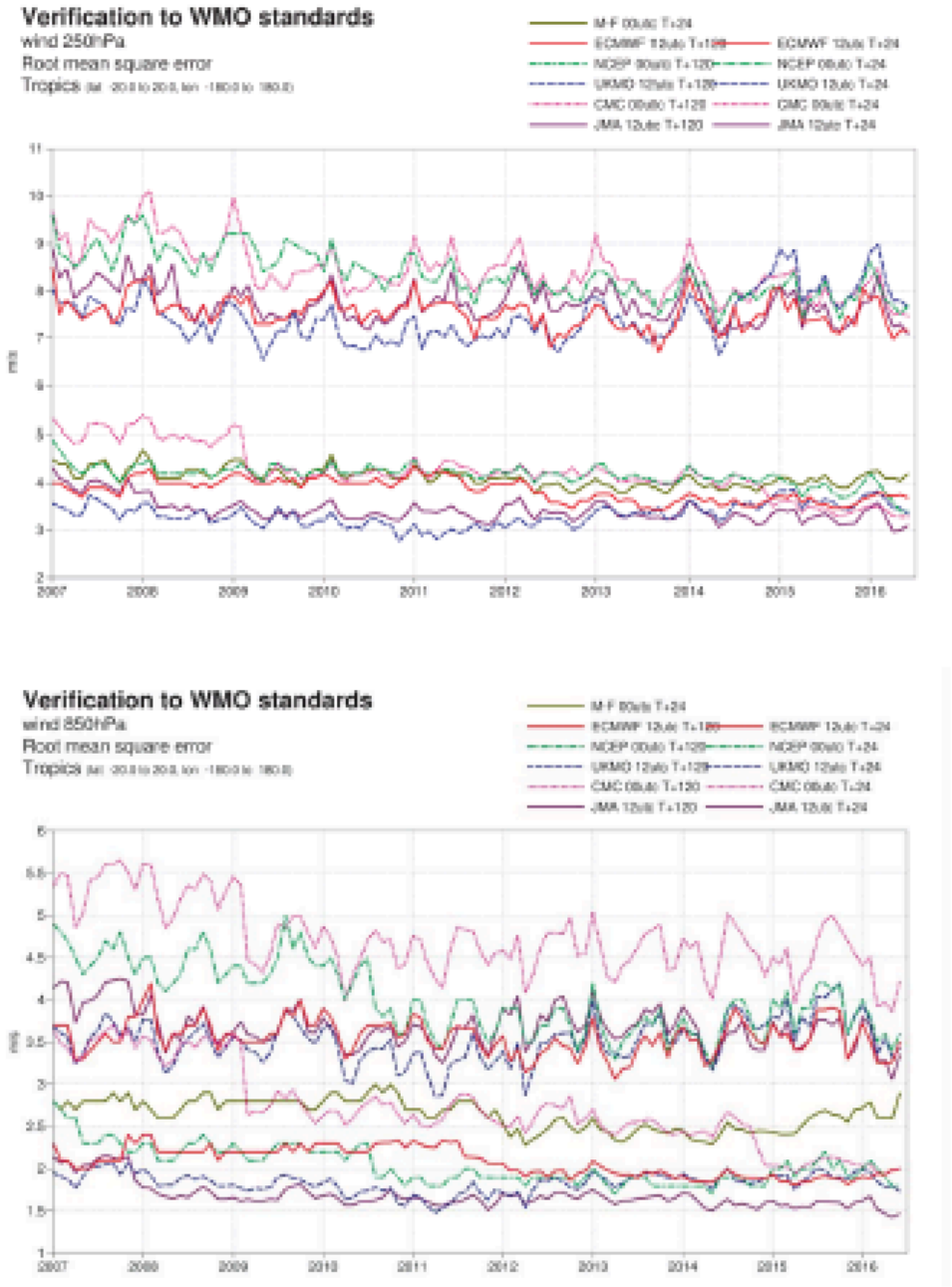

Figure 15: WMO-exchanged scores from global forecast centres. RMS vector wind error over tropics at 250 hPa (top) and 850 hPa (bottom). In each panel the upper curves show the five-day forecast error and the lower curves show the one-day forecast error. Each model is verified against its own analysis.

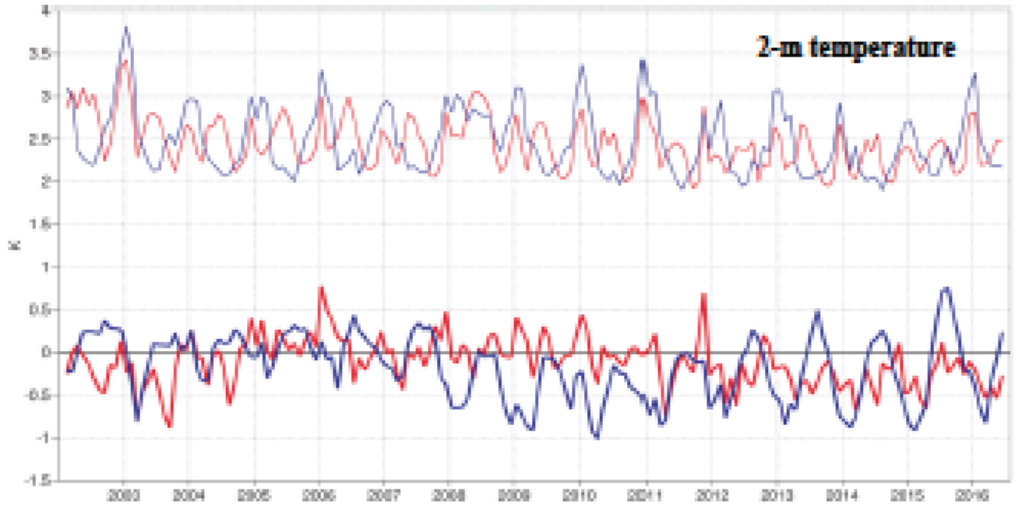

Figure 19: Verification of 2 m temperature forecasts against European SYNOP data on the GTSfor 60-hour (night-time) and 72-hour (daytime) forecasts. Lower pair of curves shows bias, upper curves are standard deviation of error.

Figure 20: Verification of 2 m dew point forecasts against European SYNOP data on the Global Telecommunication System (GTS) for 60-hour (night-time) and 72-hour (daytime) forecasts. Lower pair of curves shows bias, upper curves show standard deviation of error.

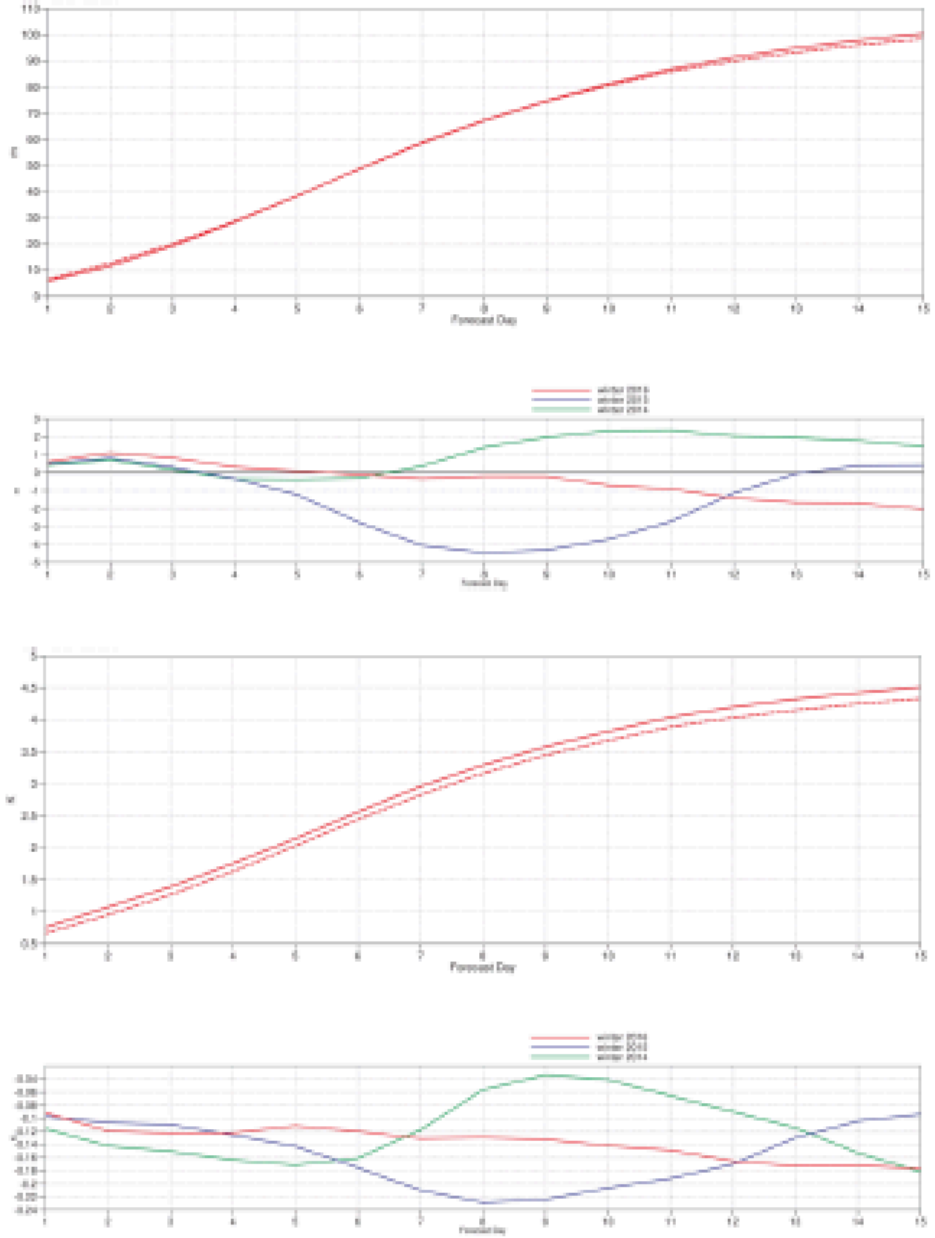

Figure 7: Ensemble spread (standard deviation, dashed lines) and RMSerror of ensemble-mean (solid lines) for winter 2015–2016 (upper figure in each panel), and differences of ensemble spread and RMSerror of ensemble mean for last three winter seasons (lower figure in each panel, negative values indicate spread is too small); verification is against analysis, plots are for 500 hPa geopotential (top) and 850 hPa temperature (bottom) over the extratropical northern hemisphere for forecast days 1 to 15.

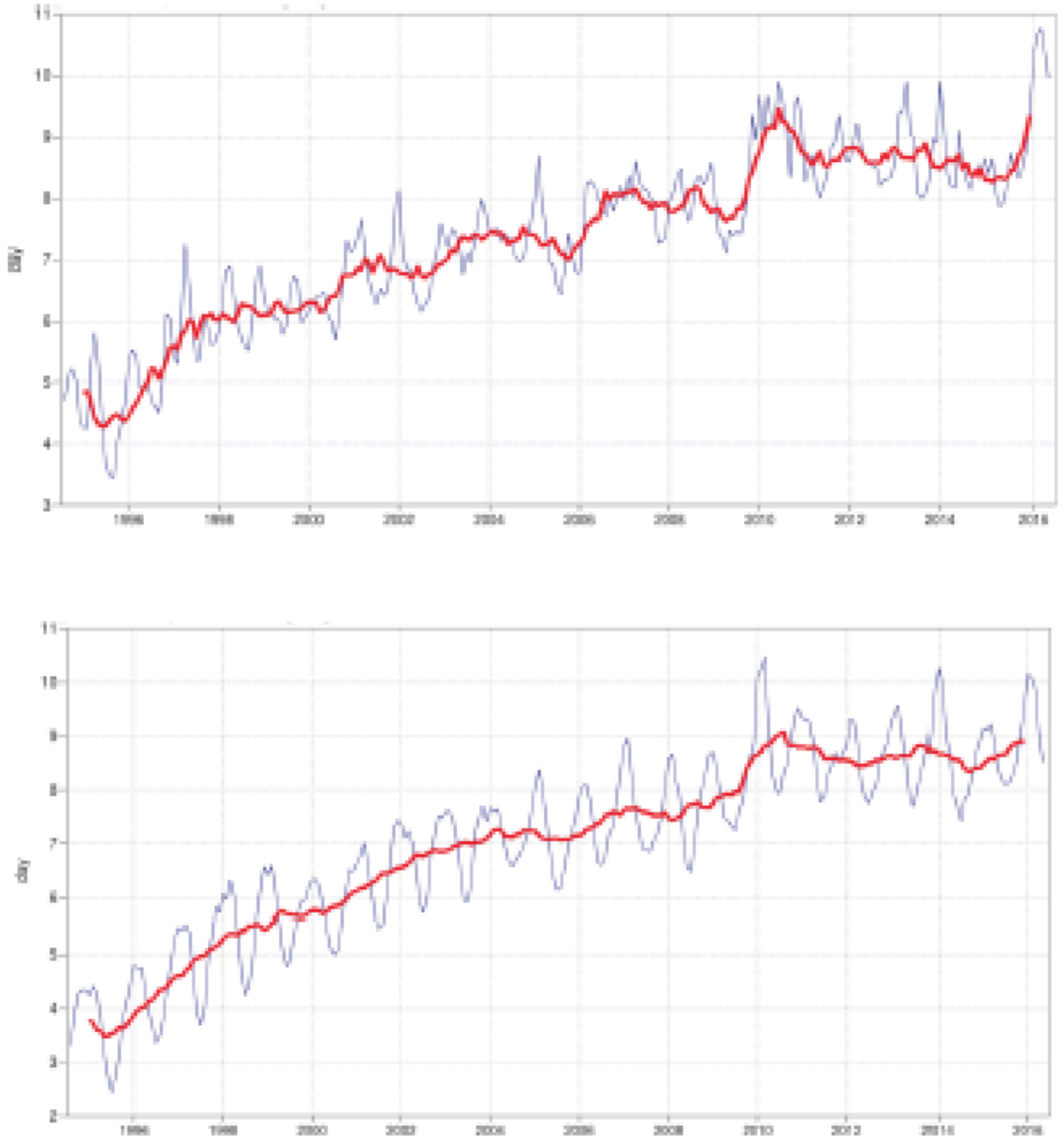

Figure 6: Primary headline score for the ensemble probabilistic forecasts. Evolution with time of 850 hPa temperature ensemble forecast performance, verified against analysis. Each point on the curves is the forecast range at which the 3-month mean (blue lines) or 12-month mean centred on that month (red line) of the continuous ranked probability skill score (CPRSS) falls below 25% for Europe (top), northern hemisphere extratropics (bottom).

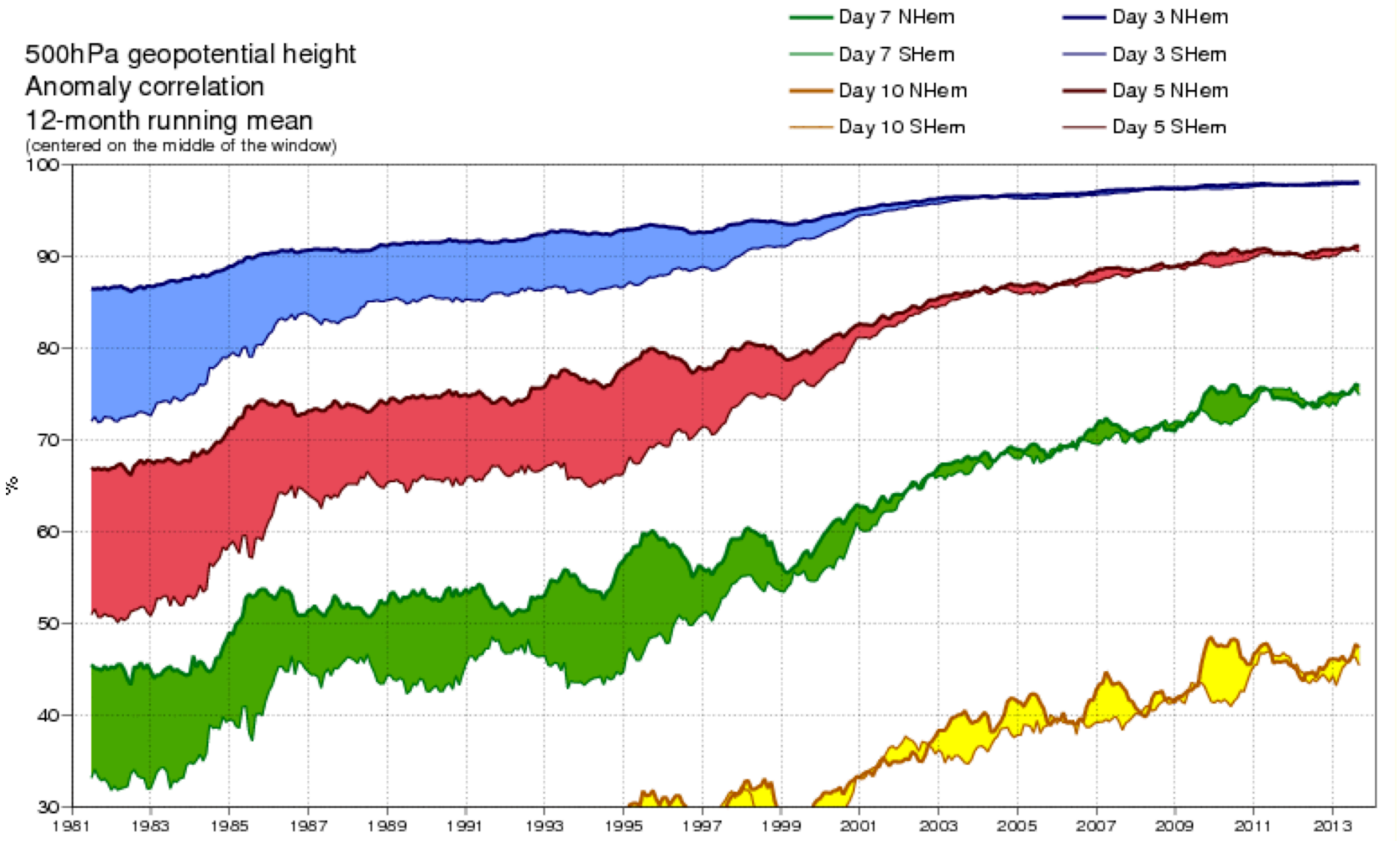
500hPa geopotential height
Anomaly correlation
12-month running mean
(centered on the middle of the window)
Day 7 NHem
Day 7 SHem
Day 10 NHem
Day 10 SHem
Day 3 NHem
Day 3 SHem
Day 5 NHem
Day 5 SHem
%
100
90
80
70
60
50
40
30
1981
1983
1985
1987
1989
1991
1993
1995
1997
1999
2001
2003
2005
2007
2009
2011
2013

Problèmes restants

- Cycle de l'eau (évaporation, condensation, influence sur le rayonnement absorbé ou émis par l'atmosphère)

- Échanges avec l'océan ou la surface continentale (chaleur, eau, quantité de mouvement, …)

- …

ECMWF

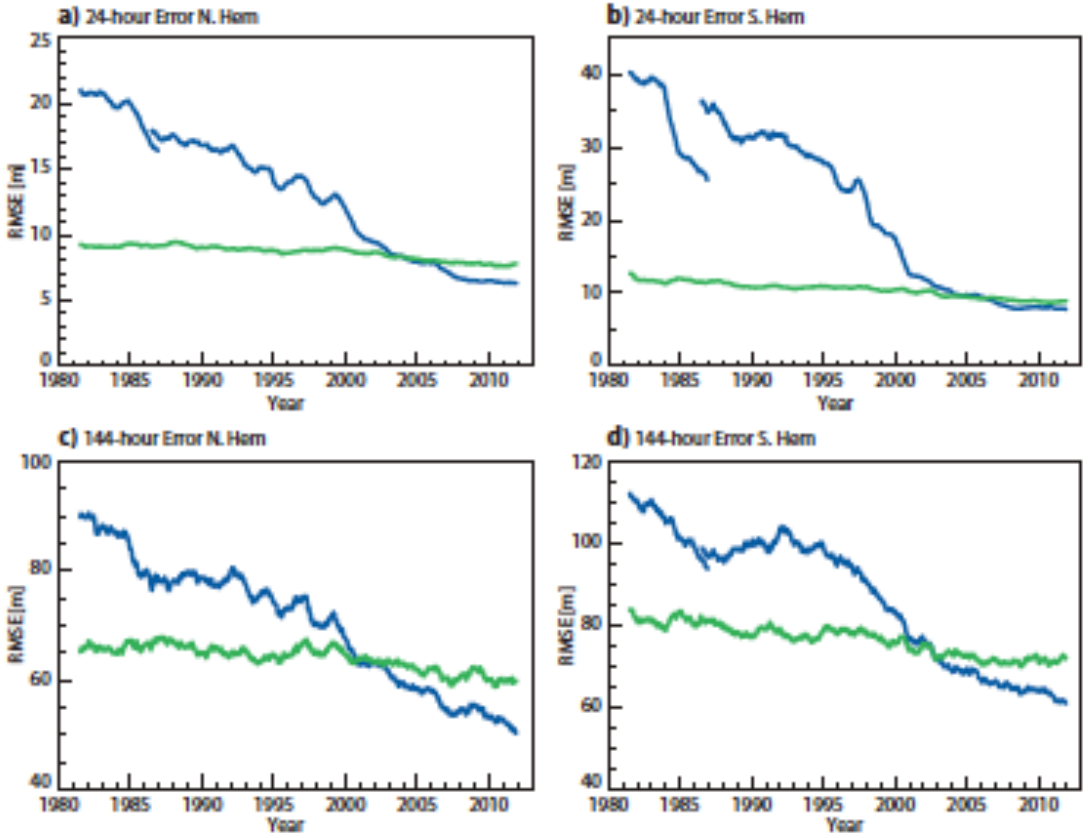

FIG. 3. Evolution of forecast errors from 1981 to 2012 for N.Hem (a and c) and S.Hem (b and d). Operational forecasts (blue) and ERA Interim (green). Note that before 1986 the operational analysis is used to verify the operational forecasts, after 1986 ERA Interim is used for the verification (with an overlap of 6 months present).

Magnusson and Källén, 2013, *Mon. Wea. Rev.*, **141**, 3142–3153

Fig. 1: Members of day 7 forecast of 500 hPa geopotential height for the ensemble originated from 25 January 1993.

Figure 6 Hurricane Katrina mean-sea-level-pressure (MSLP) analysis for 12 UTC of 29 August 2005 and t+84h high-resolution and EPS forecasts started at 00 UTC of 26 August:

1st row: 1st panel: MSLP analysis for 12 UTC of 29 Aug
2nd panel: MSLP t+84h T_L511L60 forecast started at 00 UTC of 26 Aug
3rd panel: MSLP t+84h EPS-control T_L255L40 forecast started at 00 UTC of 26 Aug
Other rows: 50 EPS-perturbed T_L255L40 forecast started at 00 UTC of 26 Aug.

The contour interval is 5 hPa, with shading patters for MSLP values lower than 990 hPa.

Why have meteorologists such difficulties in predicting the weather with any certainty ? Why is it that showers and even storms seem to come by chance, so that many people think it is quite natural to pray for them, though they would consider it ridiculous to ask for an eclipse by prayer ? […] *a tenth of a degree more or less at any given point, and the cyclone will burst here and not there, and extend its ravages over districts that it would otherwise have spared. If they had been aware of this tenth of a degree, they could have known it beforehand, but the observations were neither sufficiently comprehensive nor sufficiently precise, and that is the reason why it all seems due to the intervention of chance.*

H. Poincaré, *Science et Méthode*, Paris, 1908

(translated Dover Publ., 1952)